37. Motion Cue Effects on Pilot Tracking*

ROBERT F. RINGLAND AND ROBERT L. STAPLEFORD

Systems Technology, Inc.

The results of two successive experimental investigations of the effects of motion cues on manual control tracking tasks are reported. The first of these was an IFR single-axis VTOL roll attitude control task. Describing function data show the dominant motion feedback quantity to be angular velocity. The second experimental task was multiaxis, that of precision hovering of a VTOL using separated instrument displays with reduced motion amplitude scaling. Performance data and pilot opinion show angular position (i.e., g-vector tilt) to be the dominant cue when simulator linear motion is absent.

INTRODUCTION

Motion cues can have an important effect on several aspects of vehicular design and simulation. In this paper, attention is confined to situations involving continuous control or pilot tracking. In particular, the research reported herein was directed toward developing and validating a multimodality (both visual and motion cues) model of the human operator. The experimental portion of the research was conducted on the six-degrees-of-freedom simulator at the Ames Research Center of the National Aeronautics and Space Administration.

Two experimental programs were involved. The first of these was directed toward validating a hypothesized multimodality pilot model (to be described below) in a simple, single-axis task. The major results are in the form of pilot describing function measurements for the visual and motion modalities separately as well as together. The second program was intended to test the multimodality pilot model in a more complex, multiaxis task. The key results are in the form of performance measures and pilot opinion as a function of motion condition. In the following paragraphs we will first outline the features of the pilot model, then discuss the two experiments and the key results therefrom.

MULTIMODALITY PILOT MODEL

The basic structure of the model consists of three parallel, noninteracting feedback paths via the visual, system, the semicircular canals, and the utricles." It is recognized that the three noninteracting feedback paths are a gross simplification. However, for present purposes the simplified model is adequate.

Characteristics of the visual path are well known. A quasi-linear model for control tasks involving only visual cues is described in detail in reference 1. This description includes a describing function model form and adjustment rules for selecting the variable parameters. In the following paragraphs we will confine our attention to the characteristics of the two motion sensing paths of the model. The means by which these paths are integrated with the visual path (i.e., the adjustment rules) for a particular piloting task is inferred later in the discussions of the experimental results.

* This research was sponsored by the Man/Machine Integration Branch, Biotechnology Division, NASA-Ames Research Center, under contracts NAS2–3650 and NAS2–5261.

* Although we directly refer only to the motion sensors of the inner ear, the potential contributions of other sensors is recognized. Since the data on human motion sensing is from tests with live subjects, the contributions of all mechanisms are included.

Characteristics of the Semicircular Canal Path

While the semicircular canals are basically responsive to angular accelerations, their dynamic characteristics are such that over the range of frequencies normally used in manual control they can be considered as rate gyros which provide the pilot with a subjective impression of angular velocity. The model for the semicircular canal path can be represented by the elements shown in figure **1.** The sensor is comprised of the semicircular canals which provide the subjective angular velocity. The time constants, T_1 and T_2, are taken from a survey of the literature (ref. 2), while the threshold values shown are based upon experiments to determine the minimum detectable constant angular acceleration or step velocity change (ref. **3).** In most cases of manual control, the motions are considerably above the thresholds noted above, and the primary concern is in the frequency range of **1** to **5** rad/sec. Then the sensor dynamics for the semicircular canal path are adequately approximated by a single lag or a pure time delay as indicated in figure **1.**

The third block in figure **1** models the effects of pilot equalization and the net effects of any central processing, transmission, and neuromuscular lags. The equalization is assumed to be lead. While lag equalization is theoretically possible, the primary function of the semicircular canal path appears to be one of supplying lead equalization. Unfortunately, there are no direct data on equalization, although some of the data of reference **4** indicate that relatively large lead equalization (roughly **1** sec) is possible. Whether or not the pilot can generate lead equalization as large as that measured for visual tracking is unknown. It is hypothesized herein that the lead in the semicircular path can be as large as that used in the visual path.

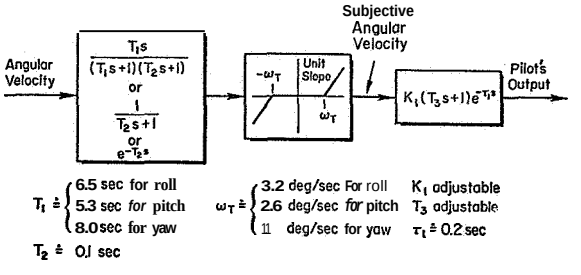

FIGURE 1.—Model for semicircular canal path.

Characteristics of the Utricular Path

The model for the utricular path consists of elements similar to those of the semicircular canal path (fig. *2).* While less data are available on the sensor dynamics of the utricles, it is widely accepted that they act like accelerometers, being sensitive to linear accelerations in the plane of the utricular maculae. This plane is inclined front end upward approximately **30** deg from the horizontal in the upright head.

The most recent data on utricular sensory dynamics is that given in reference *5.* That report suggests a model for the sensory dynamics of the form

$$\frac{\text{Subjective acceleration}}{\text{Actual acceleration}} = \frac{(T_5/T_4)(T_4 s+1)}{(T_5 s+1)(T_6 s+1)} \quad (1)$$

where

$T_4 \doteq 13$ sec
$T_5 \doteq 5.2$ sec
$T_6 \doteq 0.67$ sec.

Over the frequency range of interest in most vehicular-control situations, equation **(1)** can be adequately approximated by a single lag, as shown in figure *2.* The utricular threshold is so small, on the order of **0.01** g or less, that it will have a negligible effect in most vehicular control situations. Therefore, figure *2* shows no threshold element.

The data on possible pilot equalization forms, net lags, etc., shown in the second block of figure *2* are extremely sparse, being limited to the reference *6* analysis of some of the data from reference **3** wherein the results from one case showed the presence of a first-order lead at **3** rad/sec and a time delay of **0.3** sec. Lag equal-

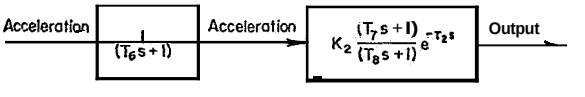

ization for certain circumstances cannot be ruled out because of the extremely wide range of acceleration numerator zeros which can occur in vehicle transfer functions. These zeros are strong functions of the vehicle stability and control properties and the pilot's location. Consequently, the model (fig. **2)** allows for both lead and lag equalization on the sensed accelerations, depending upon the piloting situation.

DESCRIPTION OF THE FIRST EXPERIMENT

The selection of the experimental task was based upon the need for sensitivity to motion cues and simplicity (i.e., single-axis task) to facilitate describing function measurement and analysis with two separate (uncorrelated) inputs. This latter feature permitted separate but simultaneous measurement of the characteristics of both the visual and motion channels.

The general task presented to the subjects was to roll stabilize a high performance VTOL which was hovering in gusty air. They were instructed to keep the roll deviations as small as possible and were given no information on their lateral position (simulator was hooded and the only display was roll angle). In response to visual (display) and motion cues, the pilot manipulated a sidestick controller. Stick position was fed to an analog computer which was used to simulate a variety of controlled element dynamics, derive the input signals to the display and the simulator, and provide a performance measure (see fig. **3).**

The controlled element dynamics were always of the form

$$Y_c = \frac{K_c}{s(s+a)} \qquad (2)$$

The data presented in this paper are for the two extreme values of a tested, 0, and **10** sec^{-1} (see ref. **7** for the complete results). Each subject was allowed to select the value of gain K_c preferred for each value of a.

For all test conditions, a disturbance input d was added to the controlled element output. This input is equivalent to the hand-off gust response of the simulated vehicle. The input was composed **of** ten sine waves and had a rms value

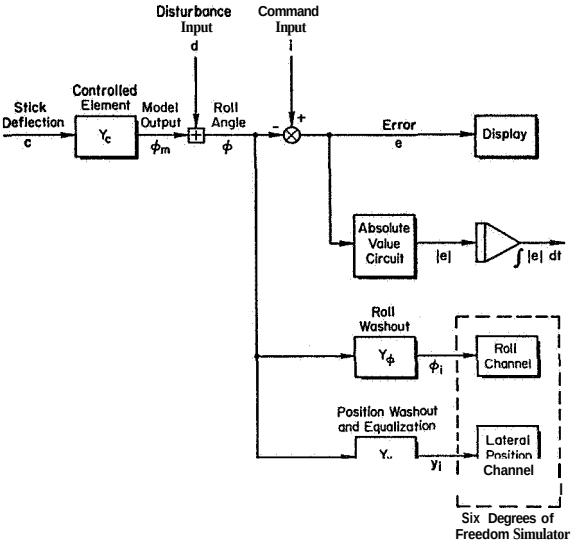

FIGURE 3.—Simulation schematic, first experiment.

of 4.3°. The amplitudes of the four highest frequency components were **1/10** those of the low frequency components.

For those runs where a separate measurement of visual and motion channels was desired, a command input i was also used, see figure **3.** The basic difference between the command and disturbance inputs is that the disturbance input feeds directly into both the display and the moving-base simulator, whereas the command feeds only into the display. Thus d tends to disturb the vehicle and the pilot attempts to cancel its effects and keep the vehicle level, while i is a roll command which the pilot attempts to follow. This input was also composed of ten sine waves of frequencies different (and thus uncorrelated with) from the frequencies of *d.* The highest five frequency components were **1/10** the amplitude of the lowest frequency components. The rms value was either **1/2** or **1/4** that of the disturbance input.

The roll angle error *e* was displayed to the pilot on a *5* in. attitude indicator (8-ball). Without the command input, the ball approximated the true horizon, i.e., the ball was nearly inertially stabilized and the cab rotated around it. The integral of the absolute value of the error was also computed to provide an on-line check on pilot performance.

A washout

$$Y_\varphi = \frac{s}{s+p_\varphi} \tag{3}$$

was used between the roll angle φ and the input to the roll channel of the six-degrees-of-freedom simulator (see fig. 3). The inverse time constant p_φ was an experimental parameter and values of 0.5, 1, and 2 sec^{-1} were tested. The data given subsequently are for the smallest value, 0.5 sec^{-1}.

The equalization between φ and the lateral position channel was used to vary the linear acceleration cues sensed by the pilot. The net transfer function between the roll angle and the input to the lateral position channel of the simulator was

$$\frac{y_i}{\varphi} = Y_y = \frac{(\ell_z - \ell_s)s^2 + bs + g}{(s+p_y)^2}. \tag{4}$$

The variables ℓ_z, b, and p, were all experimental variables, however most of the data presented herein are for the pilot's lead at the c.g. ($\ell_z = 0$), no $\dot{\varphi}$ component of acceleration ($b = 0$), and minimal washout ($p, = 0.5\ sec^{-1}$).

The data presented below are for two of the four subjects used in these experiments. The backgrounds of these two subjects are given below. They were each allowed several practice runs on the various configurations and data runs were made only after their performance, as measured by $\int |e|\, dt$, had stabilized. The data runs were approximately 4.5 min long, of which 4 min was used in the data analysis.

Subject backgrounds, first experiment.—

GB: Retired Air Force pilot; approximately 7000 hr in multi-engine aircraft.

RG: NASA research pilot; approximately 4200 hr total, mostly in single-engine fighters, 500 hr in helicopters and VTOL aircraft.

The data were originally recorded in analog form on a 14-chennel FM magnetic tape recorder. The data were subsequently sampled at 20 samples/sec and converted to a digital format. The data were then analyzed on a large-scale digital computer using the BOMM program (ref. 8) to compute describing functions.

RESULTS OF THE FIRST EXPERIMENT

When only the one input d is used, the effective loop structure is that shown in figure 4, where

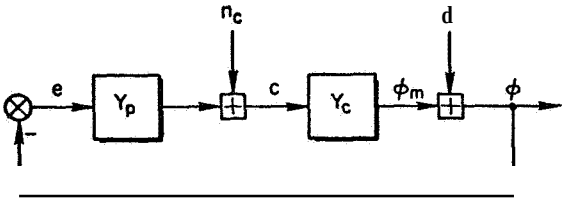

FIGURE 4.—Effective loop structure for one-input runs.

Y_p contains the combined effects of visual and motion feedbacks. The fixed-base results for some of these runs are compared with the moving-base data in figure 5 and 6 for two controlled elements. Examination of these data shows:

- The simple crossover model form of reference 1 with all its ramifications on pilot dynamic performance, adjustment rules, etc., holds for these data.
- A reduction in pilot phase lag when motion cues are added, especially for the three highest frequencies. The phase change is roughly equivalent to a time delay reduction of 0.1 to 0.2 sec.
- With less phase lag, the pilot can and does increase his mid-frequency gain and crossover frequency.
- The motion effects are somewhat different for the two subjects. In particular, the changes are somewhat less for subject GB. This may be due to his background, which is primarily in multi-engine aircraft with their slower responses and smaller motion cues.

With motion cues the crossover frequency is increased 0.5 to 1.5 rad/sec. The changes are less for $Y_c = K_c/s^2$ and less for subject GB for all controlled elements. The phase margin data show large reduction (20 to 40") with motion for $K_c/s(s+10)$, and no change for K_c/s^2. Significant phase margin reductions were not possible for K_c/s^2 as the fixed-base values were already low (5 to 15").

When both inputs are used, the loop structure is that shown in figure 7. Here Y_v is the pilot describing function for visual feedback and Ym is the describing function for motion feedback. It must be noted that Y_m actually represents the sum of two separate motion feedback channels—one angular and one linear. Furthermore, all simulator dynamics, washouts, and equalizations are included in Y_m.

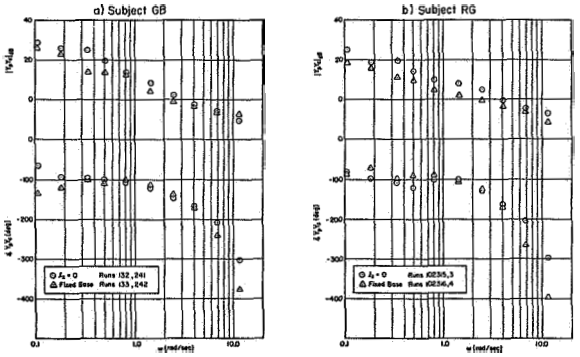

FIGURE 5.—Motion effects for $Y_c = K_c s(s+10)$.

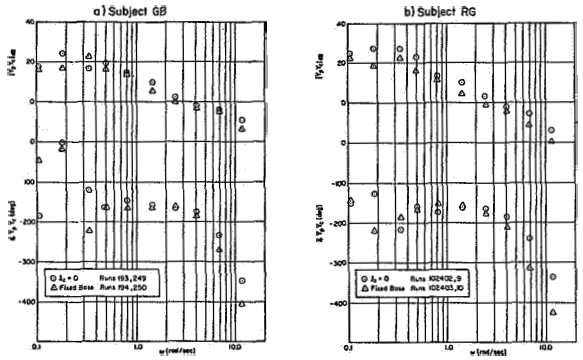

FIGURE 6.—Motion effects for $Y_c = K_c/s^2$.

The faired curves resulting from the data reduction procedure (detailed in ref. 7) are shown in figures 8 and 9. Also shown in these figures are the Y_v data for the fixed-base runs. Since the fixed-base Y_p is a visual feedback, comparison of those data and the Y_v data shows how the pilot adjusts his visual feedback when motion cues are added.

From figures 8 and 9 we see that when motion cues are present the visual feedback gain at low frequency is increased and less lead is used in the visual path, i.e., the low frequency phase lags are greater. To the extent that the semicircular canals act as rate gyros, this result might be expected. With the lead information supplied by the motion cues, the pilot does not need to supply as much visual lead as he does fixed base. He can also increase his gain and achieve a higher crossover frequency because his effective time delay is reduced.

The motion feedback describing function Y_m

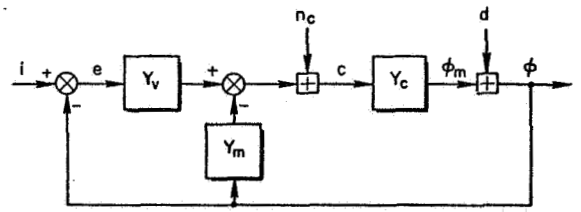

FIGURE 7.—Effective loop structure for two-input runs

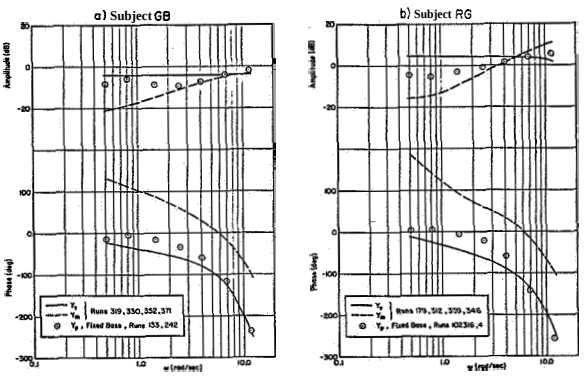

FIGURE 8.—Visual and motion feedbacks for $Y_c = K_c/s(s+10)$, $\ell_z = 0$.

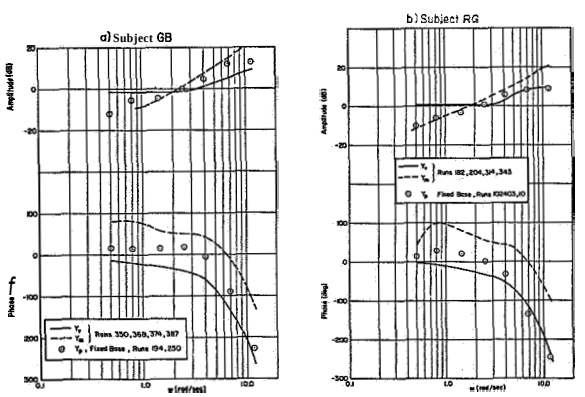

FIGURE 9.—Visual and motion feedbacks for $Y_c = K_c/s^2$, $\ell_z = 0$.

generally appears to be a very low frequency first-order lead and a time delay of roughly **0.26** sec. Comparison of the visual and motion feedbacks shows a definite difference between the two controlled elements. For $Y_c = K_c/s(s+10)$ the magnitudes of Y_v and Y_m are equal for a frequency of 5 to 9 rad/sec. For the more difficult task, $Y_c = K_c/s^2$, the magnitudes are equal at a

frequency of roughly 2 rad/sec. Thus for the task requiring more pilot lead, the relative contribution of the motion feedback is significantly higher.

It was also concluded that the motion feedback was dominantly or exclusively the angular motion. As noted above, Y_m includes simulator dynamics, washouts, and equalization. These represent known elements for both the angular and linear motion paths. If the linear motion was a significant part of the motion feedback, Y_m would not have the simple shape shown in figures 8 and 9.

In addition to the data presented above, many runs were made in which the parameters of equation (4), ℓ_z, p_y, and b, were varied, thus varying the lateral acceleration cues over a wide range. The results were negative in that the pilot describing functions show no significant change. However, the subjective impressions did change—higher lateral accelerations produced pilot complaints of a tendency toward disorientation.

Variations in the roll washout inverse time constant p_w were also tried in some of the runs. Overall describing functions for subject RG showed a slight reduction in pilot gain and therefore crossover frequency for $p_\varphi = 2$ sec^{-1}. The performance measures (integrated absolute error) showed small variations with p_w; RG's performance being degraded for $p_\varphi = 2$ sec^{-1} (which correlated with the describing function measures) and GB's performance being unaffected. This intersubject difference in part may be explained by differences in background: GB's experience is in multi-engine aircraft, while RG's is primarily in fighters. In summary, the data suggest that motion feedback via the semicircular canals is dominant and that utricular cues are relatively unimportant in the experimental tasks.

The overall results of the first experiment suggest certain additions to the multimodality pilot model as follows: For attitude tracking tasks, the overall effects of motion on the equivalent visual describing function are adjustments in the crossover frequency and effective time delay. One can use the existing quasi-linear pilot model to estimate the fixed-base pilot describing function. To allow for motion cues, one increases the crossover frequency by approximately 1 rad/sec and reduces the effective time delay by approximately 0.15 sec. This gives the overall effects of high fidelity angular cues.

The relative magnitudes of the visual and semicircular canal feedbacks depend on the controlled element dynamics; however, the visual path dominates at low frequencies and the semicircular canal path at high frequencies. For controlled elements which do not require low frequency pilot lead ($Y_c \doteq K_c/s$ in the region of crossover), the two feedbacks are of comparable magnitude in the frequency region just above crossover, 5 to 10 rad/sec. For controlled elements which do require low frequency pilot lead ($Y_c \doteq K_c/s^2$ in the region of crossover), the two feedbacks are of comparable magnitude in the frequency region just below crossover, 1.5 to 2 rad/sec. In all cases the lead provided by the angular path allows the low frequency gain of the visual path to be higher than it would be fixed-base, and the lead somewhat lower.

DESCRIPTION OF THE SECOND EXPERIMENT

The selection of the control task for the second experiment was guided, as in the first, by the need for sensitivity to the presence or absence of motion cues. Since the presence of motion cues was expected to alter the pilot's needs for visual information, his display scanning behavior was to be measured on some of the runs. With these factors in mind, a VTOL hovering task using separated instrument displays was selected.

The task presented to the subjects was to hover over a spot in mildly gusty air. They were instructed to keep their position (fore-and-aft and side-to-side) and altitude excursions to a minimum. In response to displayed visual and motion cues, the pilot manipulated a two-axis centerstick and a collective control. The controller positions were fed to an analog computer which was used to simulate the VTOL dynamics and compensate for motion simulator lags. (The displayed longitudinal position was lagged ($\tau = 0.1$ sec) to match the longitudinal response of the simulator because the latter couldn't be compensated sufficiently without introducing undesirable peaking in the simulator response.) Signals from the computer drove both the motion simulator and the displays in the simulator cap

(fig. 10). The displays consisted of an attitude ball, a CRT for display of position in the horizontal plane, and a dial gauge for display of altitude; these are similar to the conventional instrument display of reference 5. The gain on the attitude ball was five times that of the "real world" motion of the cab, and the stick gain was correspondingly reduced from typical values. This was done to keep the motion of the simulator cab within its linear excursion limits of ± 9 ft (no washouts were used in the experiment). The motions felt by the pilot were considerably attenuated from those which would otherwise be felt. Or, to put it another way, the precision of position control was considerably greater than would otherwise (attitude ball gain of 1:1) be possible in these IFR conditions."

The equations of motion for the five-degrees-of-freedom simulated VTOL are given below:

- Longitudinal

$$\begin{aligned} s(s-X_u)x+g\theta &= -X_u u_g \\ -M_u sx+s(s-M_q)\theta &= M_{\delta_e}\delta_e - M_u u_g \end{aligned} \tag{5}$$

- Lateral

$$\begin{aligned} s(s-Y_v)y-g\varphi &= -Y_v v_g \\ -L_v sy+s(s-\mathrm{L}_p)\,\varphi &= L_{\delta_a}\delta_a - L_v v_g \end{aligned} \tag{6}$$

- Vertical

$$s(s-Z_w-Z_{w'})z = Z_{\delta_c}\delta_c - Z_w w_g \tag{7}$$

- Pilot location

$$\begin{aligned} x_i &= x \\ y_i &= y \\ z_i &= z-\ell_x\theta. \end{aligned} \tag{8}$$

The intersection of the motion simulator's pitch and roll axes was the simulated center-of-gravity location of the vehicle except when ℓ_x was nonzero. Several configurations of the vehicle dynamics were tried in the course of the experiment. In this paper we shall confine our attention to the four configurations listed (in increasing order of difficulty) in Table 1—the remaining configurations involved changes in the vertical task dynamics and the pilot location as well as intermediate values of attitude damping. The dynamics are similar to those used in earlier studies (refs. 10 and 11).

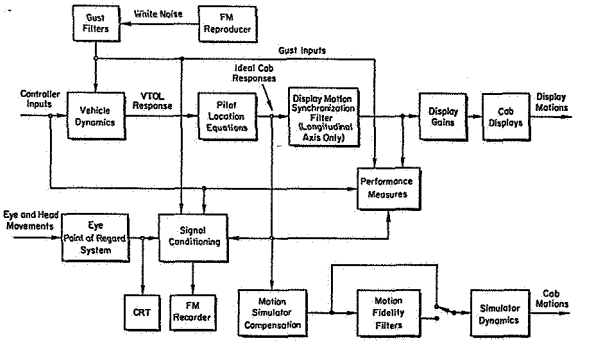

FIGURE 10.—Simulation schematic, second experiment.

TABLE 1.—VTOL *Dynamic Parameters*

Fixed parameters		
Longitudinal task	$gM_u = -0.2\ \mathrm{sec}^{-3}$,	$X_u = -0.1\ \mathrm{sec}^{-1}$
Lateral task	$gL_v = -0.2\ \mathrm{sec}^{-3}$,	$Y_v = -0.1\ \mathrm{sec}^{-1}$
Vertical task	$Z_w = -1.0\ \mathrm{sec}^{-1}$,	$Z_{w'} = -3.0\ \mathrm{sec}^{-1}$
Pilot location	$\ell_x = 0$ ft	
Variable parameters *		

Configuration	$M_q(\mathrm{sec}^{-1})$	$L_p(\mathrm{sec}^{-1})$
1	-4.0	-4.0
3	0	-4.0
4	-4.0	-0.5
6	0	-0.5

*Pilots were asked to select values of M_{δ_c}, La, and Z_{δ_c} which felt best to them for each configuration.

The three gust inputs were simulated by feeding prerecorded noise through "gust filters" having a first-order lag characteristic with $\tau = 1.0$ sec. In order to get repeatable rms level measurements (measured over a 100 sec time interval) the prerecorded noise consisted of a 100 sec white noise sample repeated over and over—a different sample for each of the three inputs. The simulated rms gust levels used were as follows (mean values are zero in all cases):

$$\sigma_{u_g} = 1.0\ \mathrm{ft/sec}$$

$$\sigma_{v_g} = 1.4\ \mathrm{ft/sec}$$

$$\sigma_{w_g} = 1.6\ \mathrm{ft/sec}.$$

Pilot ratings (based on past data, see ref. 12) are relatively insensitive to the precise level of gust excitation with the values of M_u and L_v used in this experiment.

* However, a brief test showed the position excursions could easily be kept within the limits in a VFR situation.

Three subjects were used in the second experiment, one of whom, RG, participated in the first. The backgrounds of the other two are listed below. Because of his extensive research experience and limited availability, subject RG was used as a point of reference for the other two pilots who were inexperienced in giving pilot opinion ratings and commentary.

Subject backgrounds, second experiment.—

GB: Airline flight engineer and pilot, approximately **800** hr; former USAF pilot with **650** hr as instrument instructor, approximately **4300** hr in helicopters in U.S.

EF: Airline flight engineer, approximately 200 hr; former USMC pilot with **1550** hr as primary flight instructor, **1500** hr in helicopters in Vietnam.

Subjects GB and EF were relied upon for most of the data taken. They each received **5** days of training totaling approximately **85** to 90 runs of **2** min or more duration. Nevertheless, there were still evidences of continued learning on these extremely difficult to fly configurations at the conclusion of the program.

RESULTS OF THE SECOND EXPERIMENT

The pilot performance (measured in terms of time-averaged rms motions) and opinion rating for each of the four configurations are shown in figure **11.** The pilot opinion ratings (PR) listed are to be interpreted only relative to this experiment—in the training runs it was discovered that these configurations were so difficult as to merit ratings between **8** and **10** on the Cooper-Harper scale in any motion condition. Consequently, the pilots were instructed to rate the simulation as flyable (pilot opinion rating (Cooper-Harper scale) better than **10.0)** if they were able to keep the position excursions within the motion simu-

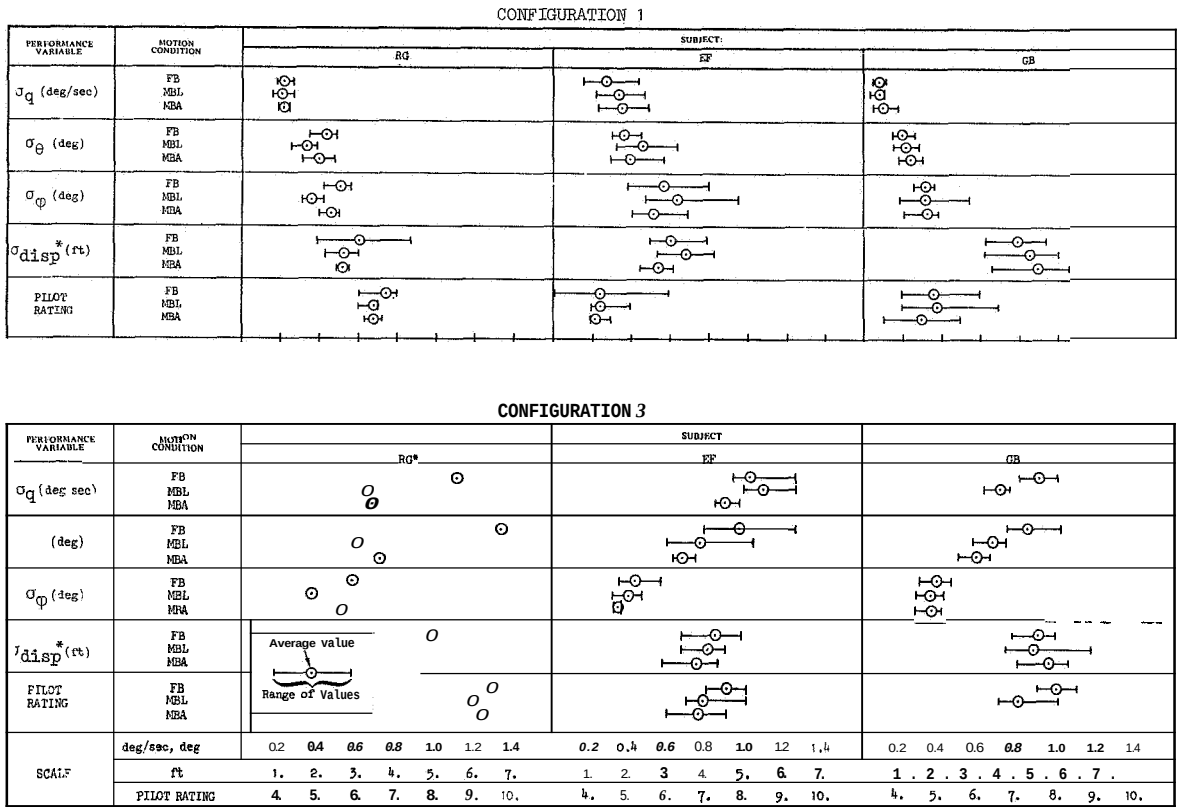

FIGURE 11.—Performance and pilot rating data.

lator limits for the duration of the run, barring momentary exceedances. This made up (at least in part) for the large rating decrement caused by the IFR conditions of the experiment. The more significant results to be drawn from these figures and the pilot commentary are as follows:

- The **MBA** motion condition (moving base, angular motion only) is rated best by all pilots for all configurations with performance

$$(\sigma_{\text{disp}} = (\sigma_x^2 + \sigma_y^2 + \sigma_z^2)^{1/2})$$

confirming this for all subjects but **GB** who is postulated to "relax"—his performance is worst and his rating best in this motion condition for all configurations.

- The **MBL** motion condition (moving base, linear and angular motion) is rated at an intermediate level between the **FB** (fixed base) and **MBA** conditions by all pilots for all configurations with the exception of the easiest (configuration 1) where EF and **GB** rate the **MBL** condition worse than **FB.** Pilot performance confirms this trend.

- Pilot commentary indicated the **MBL** condition to be subjectively "strange," "confusing," "distracting," etc., suggesting a tendency to vertigo in this motion condition. The **MBA** condition was subjectively better because of the "unmistakable" g-vector tilt cue and the absence of the "distractions," etc., of the **MBL** motion condition.

A comparison of these data with those given in reference **11,** plus comparing the data with semicircular canal thresholds (fig. 1) indicate the presence of threshold effects similar to those measured in the simpler task of reference **13.** The angular motions are so small (as a result of the display scaling used to permit position control within the simulator limits) that the ebneficial effects of motion are considerably re-

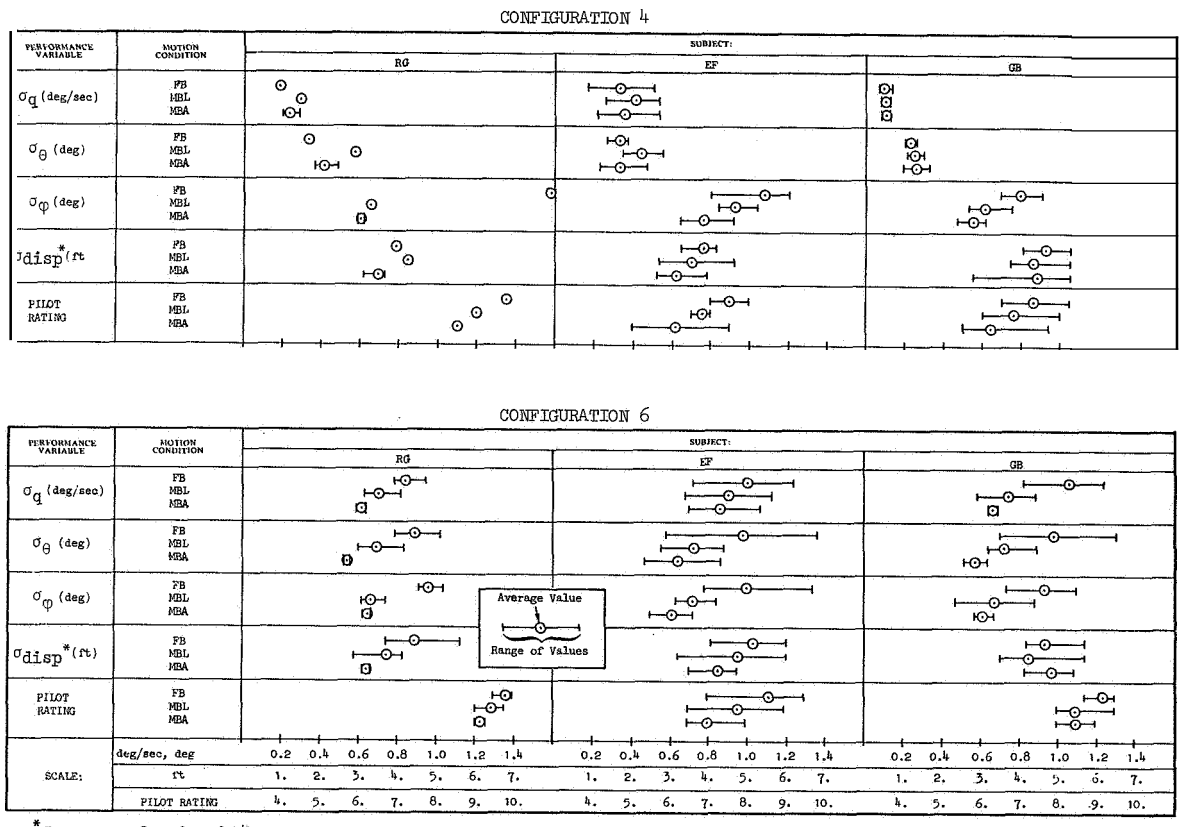

FIGURE 11.—Concluded.

duced. Thus the variation of performance (and opinion with motion condition is less than one might otherwise expect.

On several of the runs (approximately ***50)*** we measured the pilots' display scanning behavior using the eye point-of-regard system developed at Systems Technology, Inc. These raw data were reduced using the techniques on reference **14** for **35** of these runs. The reduced data are available in reference **15.**

Based upon the pilots' Commentary, one would expect them to spend more time on the attitude display, FB, and less time, MBA. Figure **12,** a small sample of the reduced EPR data, graphically shows this to be the case for RG. In this figure the shaded area inside the circles represents the fraction of the time spent looking at that instrument. The width of the arrows connecting two instruments is proportional to the fraction of all changes in the eye point-of-regard attributable to looks between the two instruments indicated. Thus, figure **12** shows that RG spends most of his time shifting his gaze back and forth between the attitude and position displays with little attention to the altitude display. The largest fraction of his time is on the attitude display in all motion conditions, although his need to look at this display is (apparently) least in the MBA condition.

By way of summarizing some of these results, table **2** shows the various cues available to the pilot in the three motion conditions investigated in the second experiment. The data presented indicate a strong preference for the angular motion only (MBA) condition over full motion (MBL). This preference is attributed to the absence of auditory cues and simulator vibration in the MBA condition relative to MBL, and/or the presence and pilot's use of the g-vector tilt cue, in the MBA condition. The latter point of view was confirmed by pilot commentary taken at face value, while the former is certainly a factor in the easiest, No. **1,** configuration, which would ordinarily be expected to show little advantage accruing to the presence of motion. The g-vector tilt cue as an indicator of attitude, present only in the MBA condition, is apparently used by the pilot in addition to his attitude display. It can give him an attitude indication when he is looking elsewhere which can be used at least to alert him to a changing situation, and perhaps even to provide some measure of closed-loop control. The apparent g-vector tilt experienced in the MBL condition is related weakly to attitude and strongly to the simulated gust excitation. It can't help him in control at attitude and, because of the restricted visual world inside the simulator cab (in particular, the absence of an approximation to a real-world display which would aid his perception of orientation), can presumably lead to vertigo. Consequently, a moving-base simulator with angular motion only gives the pilot an additional cue not present in the real world. If this cue can be used advantageously, as it apparently can in the simulated task where attitude control is of paramount importance and separated instrument displays are employed, then the results obtained will be optimistic relative to IFR flight. The multimodality pilot model in this instance includes utriclar as well as semicircular canal feedbacks, the former acting to supplement his relatively poor (in IFR conditions) perception of vehicle attitude.

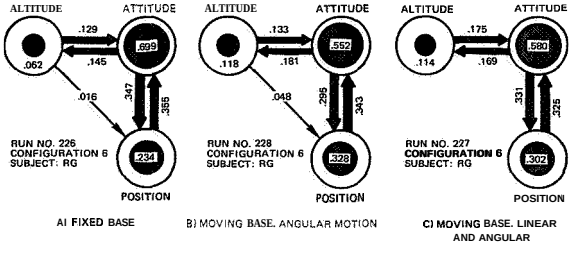

FIGURE 12.—Transition link vectors and dwell fractions.

CONCLUSIONS

In the course of the second experimental program we attempted to predict the performance to be achieved using the multimodality pilot model with adjustments for scanning workload. The predictions (detailed in ref. **15)** correctly predicted the performance trends with configuration changes and motion conditions, but were considerably wide of the mark in predicting actual performance due to a number of factors. Foremost among these were the VFR IFR difference, causing a large decrement in both performance and opinion (the existing pilot models are based upon results measured in simpler

TABLE 2.—*Simulator Motion Conditions and Pilot Sensory Modalities*

Simulator condition \ Pilot modality	Vision	Audition	Vestibular: Canals	Vestibular: Utricle	Other proprioceptive
Fixed-base	Displays				
Moving-base, angular motions only	Displays		Angular velocities near effective threshold level.	G-vector tilt. Pilot's head not at center of cab rotation (simulated c.g.)*	G-vector tilt
Moving base, angular and linear motions	Displays	Simulator rumble. Amplidyne whine (only in training and early experimental runs where motions are large).	Angular velocities near effective threshold level.	G-vector tilt *only* when linear motion limits exceeded. Pilot's head not at center of cab rotation (simulated c.g.)*	G-vector tilt only when linear motion limits exceeded. Simulator vibration in linear degrees of freedom.

* Therefore angular accelerations produce linear accelerations at pilot's head.

tasks). In addition, the predictions did not include any allowance for motion threshold effects, or for the possible benefits of utricular cues.

The lessons are clear: Certain improvements (based upon experimentation) in pilot models are required in the area of multiple display scanning behavior; the data base upon which such behavior is predicted is quite limited, see references 14, **16,** and **17.** Application of the model requires careful examination of simplifying assumptions (e.g., are motion amplitudes large enough to permit ignoring vestibular threshold effects?). Finally, additional experimentation is needed to define the extent to which threshold effects are due to simulator artifacts ("masking" effects due to noise and vibration), actual vestibular thresholds, or pilot workload (stress).

REFERENCES

1. McRuer, Duane T.; Graham, Dunstan; and Krendel, Ezra S.: Manual Control of Single-Loop Systems: Parts I and 11. J. Franklin Institute, vol. 283, no. 1, Jan. 1967, and no. 2, Feb. 1967.
2. Peters, Richard A.: Dynamics of the Vestibular System and Their Relation to Motion Perception, Spatial Disorientation, and Illusions. NASA CR-1309, Apr. 1969.
3. Meiry, Jacob L.: The Vestibular System and Human Dynamic Space Orientation. MIT, Man-Vehicle Control Lab., Thesis No. T–65–1, June 1965.
4. Shirley, Richard S.: Motion Cues in Man-Vehicle Control. MIT, Man-Vehicle Lab., Thesis No. MVT–68–1, Jan. 1968.
5. Young, L. R.; and Meiry, J. L.: A Revised Dynamic Otolith Model. 3rd Symposium on Role of the Vestibular Organs in Space Exploration (Pensacola, Fla.) Jan. 23–27, 1967.
6. Alex, F. R.: Analysis of Two Manually Controlled Compensatory Systems with Inclusion of Motion Cues. Working Paper 162–2, Systems Technology, Inc., Feb. 1967.
7. Stapleford, R. L.; Peters, R. A.; and Alex, F. R.: Experiments and a Model for Pilot Dynamics with Visual and Motion Inputs. NASA–CR–1325, May 1969.
8. Bullard, E. C.; Oglebay, F. E.; Munk, W. H.; and Miller, G. R.: A User's Guide to BOMM. Univ. of Calif. Institute of Geophysics and Planetary Physics, Jan. 1966.
9. Williams, P. R.; and Kronholm, M. B.: Technical Report on Simulation Studies of an Integrated Electronic Vertical Display, Rept. No. 1161 R 0021. United Aircraft Corp., Dec. 31, 1965.
10. Miller, D. P.; and Vinje, E. W.: Fixed-Base Flight Simulator Studies of VTOL Aircraft Handling Qualities in Hovering and Low-Speed Flight. AFFDL–TR–67–152, Jan. 1968.
11. Vinje, E. W.; and Miller, D. P.: Analytical and Flight Simulator Studies to Develop Design Criteria

for VTOL Aircraft Control Systems. AFFDL-TR-68-165, Wright-Patterson AFB, Apr. 1969.

12. CRAIG, S. J.; AND CAMPBELL, A.: Analysis of VTOL Handling Qualities Requirements. Part I: Longitudinal Hover and Transition. AFFDLTR-67-179, Wright-Patterson AFB, Oct. 1968.
13. BERGERON, H. P.; ADAMS, J. P.; AND HUNT, G. J.: The Effects of Motion Cues and Motion Scaling on One- and Two-Axis Compensatory Control Tasks. NASA TN D-6110, Jan. 1971.
14. WEIR, DAVID H.; AND KLEIN, RICHARD H.: The Measurement and Analysis of Pilot Scanning and Control Behavior During Simulated Instrument Approaches. NASA CR-1535, June 1970.
15. RINGLAND, R. F.; STAPLEFORD, R. L.; AND MAGDALENO, R. E.: Motion Effects on an IFR Hovering Task—Analytical Predictions and Experimental Results. Tech. Rept. No. 188-1, Systems Technology, Inc., Oct. 1970.
16. ALLEN, R. W.; CLEMENT, W. F.; AND JEX, H. R.: Research on Display Scanning, Sampling, and Reconstruction Using Separate Main and Secondary Tracking Tasks. NASA CR-1569, July 1970.
17. CLEMENT, W. F.; AND HOFMANN, L. G.: A Systems Analysis of Manual Control Techniques and Display Arrangements for Instrument Landing Approaches in Helicopters. Vol. I: Speed and Height Regulation. Tech. Rept. 183-1, Systems Technology, Inc., July 1969.